

# Deconstructing Superconductivity

Dylan Albrecht,<sup>\*</sup> Christopher D. Carone,<sup>†</sup> and Joshua Erlich<sup>‡</sup>

*High Energy Theory Group, Department of Physics,  
College of William and Mary, Williamsburg, VA 23187-8795*

(Dated: August 2012)

## Abstract

We present a dimensionally deconstructed model of an  $s$ -wave holographic superconductor. The 2+1 dimensional model includes multiple charged Cooper pair fields and neutral exciton fields that have interactions governed by hidden local symmetries. We derive AdS/CFT-like relations for the current and charge density in the model, and we analyze properties of the Cooper pair condensates and the complex conductivity.

arXiv:1208.2700v2 [hep-th] 21 Aug 2012

---

<sup>\*</sup>djalbrecht@email.wm.edu

<sup>†</sup>cdcaro@wm.edu

<sup>‡</sup>jxerli@wm.edu

## I. INTRODUCTION

High- $T_c$  superconductors continue to fascinate physicists, both for their technological prospects and for their unconventional physical properties. Discovered in 1986 [1], high- $T_c$  superconductors have superconducting transition temperatures  $T_c$  higher than the upper limit of around 30 K suggested by the BCS theory [2], and the mechanism of superconductivity in these materials remains uncertain. High- $T_c$  superconductors are Type II, allowing magnetic fields to penetrate in conjunction with Abrikosov vortex currents which maintain localized magnetic fluxes. A number of features of high-temperature superconductors remain poorly understood, including the existence of a pseudogap phase in which a gap in the excitation spectrum opens up at temperatures above the superconducting transition [3], and a thermoelectric Nernst effect that occurs in both the superconducting and pseudogap phases [4]. A few additional classes of exotic high- $T_c$  superconductors have recently been discovered, including the iron pnictides [5], and research into their properties is ongoing.

In the absence of a clear theoretical understanding of high- $T_c$  superconductors and other systems with strongly correlated electrons, it is useful to explore simplified models which describe similar phenomenology. It has long been understood that certain relativistic field theories describe a variety of phenomena typical of superconductors. In the Abelian Higgs model, a charged scalar field condenses while the photon becomes massive, in analogy to the condensation of Cooper pairs and the consequent expulsion of magnetic fields from superconducting materials. The Abelian Higgs model also has Nielsen-Olesen vortex solutions which maintain localized magnetic flux tubes [6], much like the Abrikosov vortices in Type II superconductors.

One approach that has stimulated much effort especially from the string theory community is the use of the AdS/CFT correspondence [7], which relates certain strongly coupled field theories to gravitational systems in higher-dimensional spacetime backgrounds. Due to the extra-dimensional nature of these models they are referred to as holographic. There is a mapping between observables in the superconducting system and fields in the corresponding extra-dimensional model. Progress has been made in understanding properties of holographic models of superconductors and other condensed matter systems, including  $s$ ,  $p$ , and  $d$ -wave superconductivity [8–10], the Nernst effect in the quantum critical regime [11], strange metallic behavior [12], enhancement of the superconducting gap compared to BCS

theory [13], and Homes’s empirical law for  $T_c$  as a function of low-temperature superfluid density and normal-phase resistivity [14, 15]. In some models of holographic superconductors there is no hard zero-temperature gap [16]. For some reviews on holographic models of condensed matter systems, see Refs. [13, 17, 18].

In parallel to the development of the AdS/CFT correspondence in string theory, extra-dimensional model building has led to the discovery of new paradigms for gravitational physics [19, 20], electroweak symmetry breaking [21], grand unification [22], and other possible new physics. Notably, in order to define these otherwise nonrenormalizable extra-dimensional gauge theories, a procedure was developed for dimensionally “deconstructing” extra-dimensional theories into renormalizable field theories defined in the natural (lower) dimension of the system of interest [23]. At long distances, a deconstructed model is effectively described by the corresponding extra-dimensional theory, latticized in the extra dimension(s). In some models the number of effective lattice sites can be taken as small as just two or three while retaining the desirable features of the extra-dimensional theory. Deconstruction provides a systematic procedure for finding relatively simple, weakly coupled models of interesting physical systems, in the number of dimensions that naturally characterizes the system of interest [24].

In this paper we present and analyze a deconstructed model of the simplest holographic superconductor, the Abelian Higgs model in 3+1 dimensional<sup>1</sup> Anti-de Sitter-Schwarzschild spacetime (AdS<sub>4</sub>-Schwarzschild), which is intended to model *s*-wave superconductors in 2+1 dimensions [9]. Superconductivity in the cuprates is along two-dimensional CuO<sub>2</sub> planes, so the hope is that a model with two spatial dimensions will capture some of the relevant physics in these systems. The deconstructed model is a 2+1 dimensional model in which Maxwell’s electrodynamics is replicated a number of times. Fields charged under pairs of the electromagnetic U(1) gauge groups condense, giving rise to the latticized extra-dimensional structure of the model. The temperature-dependent couplings of the Maxwell fields are rotationally invariant but not Lorentz invariant. Additional charged fields representing Cooper pair operators condense in the superconducting phase, and the combined effects of the multiple condensates determine the properties of the superconductor. The electron pair

---

<sup>1</sup> The +1 in the spacetime dimensionality always refers to time, not the extra spatial dimension of the holographic model.

wavefunctions in high- $T_c$  superconductors are thought to have more complicated symmetry than the  $s$ -wave described by scalar Cooper pair fields, so the present model is not expected to capture features sensitive to the symmetry of the wavefunctions.

The deconstructed model helps to elucidate certain aspects of holographic superconductivity and suggests the relevant effective degrees of freedom in physical realizations of these superconductors. One generic feature of this class of models is the existence of hidden local symmetries [25] and corresponding neutral excitations, much like the vector mesons of Quantum Chromodynamics. Such excitations in the superconductor may be interpreted as excitons<sup>2</sup>, electron-hole bound states which can be created when a photon is absorbed by certain materials [26]. In analogy to a deconstructed holographic model of hadrons [27], we derive discretized AdS/CFT relations between bulk and boundary observables. We analyze properties of the superconducting transition and the frequency-dependent conductivity as the number of extra-dimensional lattice sites, and correspondingly the number of pair condensates and exciton fields, is reduced.

In Sec. II, we review the Abelian Higgs model in the AdS<sub>4</sub>-Schwarzschild spacetime as a model of superconductivity in two spatial dimensions. In Sec. III, we describe the deconstructed model and explain the calculation of observables of interest. In Sec. IV, we present numerical results. We conclude with a discussion and suggestions for future research in Sec. V.

## II. CONTINUUM MODEL

In this section we review the holographic model that will be deconstructed in Sec. III. Much of the content of this section is a summary of results contained elsewhere, for example in Ref. [9], though we generalize certain results for the sake of comparison with the deconstructed model.

The starting point is a vacuum solution to Einstein's equations with negative cosmological constant in 3+1 dimensions, namely the AdS<sub>4</sub>-Schwarzschild solution. The spacetime is

---

<sup>2</sup> The neutral, spin-1 excitations might more appropriately be identified with polaritons, if there were a dynamical photon in the deconstructed theory that mixed strongly with these excitons.

described by a metric of the form

$$ds^2 = F(r)dt^2 - r^2(dx^2 + dy^2) - \frac{1}{F(r)}dr^2, \quad (2.1)$$

where

$$F(r) = \frac{r^2}{L^2} \left( 1 - \frac{r_H^3}{r^3} \right). \quad (2.2)$$

The constant  $L$  is the Anti-de Sitter scale, which we will often set to 1. We refer to coordinates in which the metric takes the form of Eq. (2.1) as  $r$  coordinates, and the coordinate  $r$  runs from  $r_H$  to  $\infty$ . The 2+1 dimensional surface at  $r = \infty$  is referred to as the ultraviolet (UV) boundary, and the surface at  $r = r_H$  is the horizon. The AdS/CFT correspondence suggests the identification of the temperature of the material with the Hawking temperature of the AdS black hole, namely

$$T = 3r_H/(4\pi L^2). \quad (2.3)$$

With nonvanishing charge density the relevant background spacetime is instead the AdS-Reissner-Nordstrom spacetime, a charged solution to the Einstein-Maxwell equations with a negative cosmological constant. However, in this paper we neglect the backreaction of the charge density on the geometry. In this approximation the spacetime metric continues to take the form of Eqs. (2.1) and (2.2), even when the solutions of interest have nonvanishing charge density.

The holographic model contains a U(1) gauge field corresponding to electromagnetism, and a charged scalar field corresponding to the Cooper pairs. The model is translationally invariant in 2 spatial dimensions, and is therefore not expected to reproduce phenomena that are sensitive to the atomic lattice.

The action for the model is given by

$$S = \int d^4x \sqrt{g} \left\{ -\frac{1}{4} F_{MN} F^{MN} + |(\partial_M - iA_M)\psi|^2 - m^2|\psi|^2 \right\}, \quad (2.4)$$

where index contractions are with the 4D metric  $g_{MN}$ , and  $g = |\det g_{MN}|$ .

The action in  $r$  coordinates has the form

$$S = \int d^3x dr r^2 \left\{ \frac{1}{2r^2 F(r)} (F_{0a})^2 - \frac{1}{4} r^{-4} (F_{ab})^2 + \frac{1}{2} (F_{0r})^2 - \frac{F}{2r^2} (F_{ar})^2 + \frac{1}{F(r)} |(\partial_0 - iA_0)\psi|^2 - r^{-2} |(\partial_a - iA_a)\psi|^2 - F(r) |(\partial_r - iA_r)\psi|^2 - m^2|\psi|^2 \right\}. \quad (2.5)$$

Here  $F_{MN} = \partial_M A_N - \partial_N A_M$  is the field strength of the U(1) gauge field, and the charge of the field  $\psi$  is normalized to 1. Our convention is that Latin indices  $a, b, \text{etc.}$ , represent

spatial components  $x$  or  $y$ . We have explicitly shown the metric factors in Eq. (2.5), so remaining index contractions are taken with the Kronecker delta  $\delta_{MN}$ . According to the AdS/CFT correspondence the mass  $m$  is related to the scaling dimension of the operator related to  $\psi$ , and for definiteness we will assume  $m^2 = -2/L^2$  as in Ref. [9], corresponding to a Cooper pair operator of dimension 2 (or 1, as discussed below).

Defining  $\phi \equiv A_0$  as in Ref. [9], and considering solutions with  $\psi = \psi(r)$ ,  $\phi = \phi(r)$  and  $A_a = 0$ , the coupled equations of motion for  $\psi$  and  $\phi$  in the gauge where  $A_r = 0$  are

$$\psi'' + \left( \frac{F'(r)}{F(r)} + \frac{2}{r} \right) \psi' + \frac{\phi^2}{F(r)^2} \psi - \frac{m^2}{F(r)} \psi = 0, \quad (2.6)$$

$$\phi'' + \frac{2}{r} \phi' - \frac{2|\psi|^2}{F(r)} \phi = 0. \quad (2.7)$$

Near the UV boundary, the solutions behave as [9],

$$\psi = \frac{\psi^{(1)}}{r} + \frac{\psi^{(2)}}{r^2} + \dots, \quad (2.8)$$

$$\phi = \mu - \frac{\rho}{r} + \dots. \quad (2.9)$$

The time component of the gauge field couples to the charge density, so the AdS/CFT correspondence identifies  $\mu$  with the electric chemical potential and  $\rho$  with the charge density. For the Cooper pair operator there are two choices: either  $\psi^{(1)}$  acts as a source and  $\psi^{(2)}$  corresponds to the expectation value of the Cooper pair operator, or *vice versa*. This choice determines the scaling dimension of the Cooper pair operator according to the AdS/CFT correspondence. For definiteness we will choose to take  $\psi^{(1)}$  as the source of the Cooper pair operator  $O_2$ , which then has mass dimension two; the other choice would correspond to an operator of dimension 1. The Cooper pair operator should only be turned on dynamically, so vanishing of its source becomes a UV boundary condition,  $\psi^{(1)} = 0$ . Additional boundary conditions are  $\phi(r_H) = 0$  for regularity of the solution and  $\phi(\infty) = \mu$ . The equations of motion enforce the condition  $F'(r)\psi'(r) = m^2\psi(r)$  at the horizon if  $\psi(r)$  is finite, so the additional boundary condition on  $\psi$  at the horizon is replaced with a regularity condition.

In order to study the response of our system to an oscillating electric field, we consider solutions for which  $A_x$  oscillates in time,  $A_y = A_r = 0$  and  $A_0$  behaves as in Eq. (2.9). Assuming the form

$$A_x(t, r) = e^{-i\omega t} A(r), \quad (2.10)$$

the bulk equation of motion for  $A_x$  has the form,

$$-\frac{\omega^2}{F(r)}A(r) - \frac{d}{dr}(F(r)A'(r)) + 2A(r)|\psi(r)|^2 = 0. \quad (2.11)$$

For large  $r$  the solutions for  $A_x$  have the form

$$A_x = A_x^{(0)} + A_x^{(1)}/r + \dots. \quad (2.12)$$

According to the AdS/CFT correspondence,  $A_x^{(0)}$  acts as the source for the current  $j^x$  and hence corresponds to a background electric field  $E_x = \partial_t A_x^{(0)}$ . The AdS/CFT correspondence also suggests an identification of the normalizable component  $A_x^{(1)}$  with (minus) the current  $j^x$  in the given background state [28]. In Sec. III, we explain how this identification arises in the deconstructed model. Hence, we can write<sup>3</sup>

$$\begin{aligned} E_x &= \partial_t A_x|_{r \rightarrow \infty} = -i\omega A_x|_{r \rightarrow \infty}, \\ j^x &= -A_x^{(1)} = r^2 \partial_r A_x|_{r \rightarrow \infty}. \end{aligned} \quad (2.13)$$

The conductivity  $\sigma$  is therefore determined in the holographic model by

$$\sigma = \frac{j^x}{E_x} = \frac{r^2 A'(r)}{-i\omega A(r)} \Big|_{r \rightarrow \infty}, \quad (2.14)$$

### A. The Normal Phase

At temperatures greater than  $T_c$  the charged field  $\psi$  vanishes, in which case solutions of the following first order equations also solve Eq. (2.11):

$$A'_\pm(r) = \pm \frac{i\omega}{F(r)} A_\pm(r). \quad (2.15)$$

The solutions are

$$\begin{aligned} A_\pm(r) &= \exp \left\{ \pm i\omega \int \frac{dr}{F(r)} \right\} \\ &= \exp \left\{ \pm \frac{i\omega}{6r_H} \left( 2\sqrt{3} \tan^{-1} \left[ \frac{2r + r_H}{\sqrt{3}r_H} \right] + \log \left[ \frac{(r - r_H)^2}{r^2 + rr_H + r_H^2} \right] \right) \right\}, \end{aligned} \quad (2.16)$$

and the generic solution to Eq. (2.11) is a linear combination  $A(r) = c_+ A_+(r) + c_- A_-(r)$  with constants  $c_+$  and  $c_-$ . The choice of branch of the inverse tangent and the logarithm in

---

<sup>3</sup> The sign differences in these expressions compared with Ref. [9] are due to differences in convention related to the signature of the metric. We follow the conventions of Jackson's *Classical Electrodynamics* [29].

Eq. (2.16) determines an  $\omega$ -dependent constant multiplying each of the two solutions, which can be absorbed in the coefficients  $c_+$  and  $c_-$ . The solution  $A_-(r)$  describes a wave flowing into the black hole horizon, and  $A_+(r)$  describes an outgoing wave. Son and Starinets have advocated the choice of ingoing-wave solution as a boundary condition at the horizon, based on the requirement of causality of correlators calculated by the AdS/CFT correspondence [30]. For now, we explore the consequences of the generic solution, for guidance as to what to expect from the deconstructed model. A natural choice for the boundary condition in the discretized theory is more ambiguous because causality may be imposed at the level of the lower-dimensional theory, without regards to the effective higher-dimensional description.

The complex conductivity as a function of frequency distinguishes the normal and superconducting phases. A hallmark of perfect conductivity is a delta function in the real part of the conductivity at zero frequency which, by the Kramers-Kronig relation for the conductivity, is tantamount to a zero-frequency pole in the imaginary part. The Kramers-Kronig relation follows from the assumption that correlations are causal. As a consequence, the conductivity  $\sigma(\omega)$ , which by definition is the Fourier transform of the response function relating the current to a background electric field, is analytic in the upper half plane. The Kramers-Kronig relation is then the statement of Cauchy's integral theorem for the following integral:

$$\oint_C \frac{\sigma(\omega')}{\omega' - \omega} d\omega' = \mathcal{P} \int_{-\infty}^{\infty} \frac{\sigma(\omega')}{\omega' - \omega} d\omega' - i\pi \sigma(\omega) = 0, \quad (2.17)$$

where the contour  $C$  spans the real axis above the pole at  $\omega' = \omega$  and closes in the upper half plane, and  $\mathcal{P}$  represents the principal value of the integral. The conductivity  $\sigma(\omega)$  is assumed to fall off in the upper half plane faster than  $1/|\omega|$ , so that that integral over the contour at infinity vanishes. As a consequence of Eq. (2.17), if the real part of  $\sigma(\omega)$  has a delta-function at  $\omega = 0$  then the imaginary part has a pole at  $\omega = 0$ , and *vice versa*.

It follows from Eqs. (2.14) and (2.15) that when  $\psi$  vanishes, the zero-frequency pole in  $\text{Im } \sigma$  is generically absent; the holographic description indeed describes a non-superconducting phase when the condensate vanishes, for a generic choice of boundary condition at the horizon. Note that for both the ingoing-wave and outgoing-wave solutions, the normal-phase conductivity is independent of  $\omega$ :  $\sigma = +1$  for the ingoing wave, and  $\sigma = -1$  for the outgoing wave. This result provides a phenomenological motivation for the ingoing-wave boundary conditions: the outgoing-wave solution would describe an unusual situation



in which the current produced by an electric field points in the direction opposite to the electric field. Note also that the conductivity in this model does not indicate the existence of a pseudogap phase, and does not fall off at large  $\omega$  due to relaxation as in ordinary materials.

For the generic solution for  $A_x$  with vanishing  $\psi$  and with the identification  $r_H = 4\pi T/3$ , Eq. (2.14) gives the normal-phase conductivity:

$$\sigma(\omega) = \frac{c_- \exp\left(\frac{-i\sqrt{3}\omega}{8T}\right) - c_+ \exp\left(\frac{i\sqrt{3}\omega}{8T}\right)}{c_- \exp\left(\frac{-i\sqrt{3}\omega}{8T}\right) + c_+ \exp\left(\frac{i\sqrt{3}\omega}{8T}\right)}. \quad (2.18)$$

The real part of the conductivity is then,

$$\text{Re}\sigma(\omega) = \frac{|c_-|^2 - |c_+|^2}{|c_-|^2 + |c_+|^2 + c_- c_+^* e^{-\frac{i\sqrt{3}\omega}{4T}} + c_+ c_-^* e^{\frac{i\sqrt{3}\omega}{4T}}}, \quad (2.19)$$

which oscillates as a function of  $\omega/T$  around  $\sigma = 1$  for constant  $|c_+| \ll |c_-|$ .

## B. The Superconducting Phase

For small enough  $T$ , the coupling between  $\phi$  and  $\psi$  leads to an instability which turns on the Cooper pair condensate  $\langle O_2 \rangle$ . The condensate depends on the chemical potential  $\mu$  and the charge density  $\rho$  determined by the solution to the coupled equations of motion. As argued in Ref. [9], the critical temperature scales as  $\rho^{1/2}$ . Near  $T_c$  the condensate behaves as  $\langle O_2 \rangle \propto (1 - T/T_c)^{1/2}$ . The complex conductivity for generic  $T < T_c$  has a delta function at  $\omega = 0$  and a gap  $\omega_g$ , as expected for typical superconductors, but with  $\omega_g/T_c \approx 8$  [9], significantly larger than the BCS prediction  $\omega_g/T_c \approx 3.5$ . The phenomenology of the deconstructed model has similarities to that of the continuum theory, even with only a few lattice sites, as we will see in Sec. IV.

## III. DECONSTRUCTION

In the deconstructed model we will define coordinates differently, replacing  $r$  with a new coordinate  $z = 1/r$ . In  $z$  coordinates, the extra dimension corresponds to a finite coordinate interval. The metric in  $z$  coordinates has the form

$$ds^2 = \frac{1}{z^2} \left[ f(z) dt^2 - \frac{1}{f(z)} dz^2 - (dx^2 + dy^2) \right], \quad (3.1)$$

where

$$f(z) = \frac{1}{L^2} \left( 1 - \frac{z^3}{z_H^3} \right), \quad (3.2)$$

where  $z$  runs from 0 to  $z_H$ . The surface  $z = 0$  is the ultraviolet boundary, and  $z = z_H$  is the horizon. One should keep in mind that results are coordinate independent in the continuum model, but away from the continuum limit, deconstructed models depend on the choice of coordinates in which their extra-dimensional parent model is defined.

In  $z$  coordinates, the action in the continuum theory takes the form

$$S = \int d^4x \left\{ \frac{1}{2} F_{0z}^2 + \frac{1}{2f} F_{0a}^2 - \frac{f}{2} F_{za}^2 - \frac{1}{4} F_{ab}^2 + \frac{1}{z^2 f} |\partial_0 \psi - i A_0 \psi|^2 - \frac{f}{z^2} |\partial_z \psi - i A_z \psi|^2 - \frac{1}{z^2} |\partial_a \psi - i A_a \psi|^2 - \frac{1}{z^4} m^2 |\psi|^2 \right\}, \quad (3.3)$$

where repeated  $a$  or  $b$  indices are summed over the spatial coordinates  $x$  and  $y$ . As before, we use the notation of Ref. [9], where we define  $\phi \equiv A_0$ . We replace the  $z$  axis by a lattice of  $N$  points,

$$z_j = \begin{cases} \epsilon + (j-1)a & \text{for } j = 1 \dots N-1 \\ \epsilon + (N-2)a + a_H & \text{for } j = N \end{cases}, \quad (3.4)$$

where  $z_N = z_H$  and  $\epsilon$  is a UV cutoff. The lattice spacing  $a_j$  between the  $j$  and  $j+1^{\text{th}}$  lattice sites is therefore  $a$  for  $j = 1 \dots N-2$  and  $a_H$  for  $j = N-1$ . We give ourselves the freedom to vary  $a_H$  away from  $a$  to test the sensitivity of our results to the density of sites nearest to the horizon. The discretized action is given by

$$S = \sum_{j=1}^{N-1} a_j \int d^3x \left\{ \frac{1}{2} (\partial_0 A_{z_j} - \phi'_j)^2 + \frac{1}{2f_j} (F_{0a})_j^2 - \frac{f_j}{2} (\partial_a A_{z_j} - A'_{aj})^2 - \frac{1}{4} (F_{ab})_j^2 + \frac{1}{z_j^2 f_j} |\partial_0 \psi_j - i \phi_j \psi_j|^2 - \frac{f_j}{z_j^2} |\psi'_j - i A_{z_j} \psi_j|^2 - \frac{1}{z_j^2} |\partial_a \psi_j - i A_{aj} \psi_j|^2 - \frac{1}{z_j^4} m^2 |\psi_j|^2 \right\}, \quad (3.5)$$

where  $f_j \equiv f(z_j)$ . We define derivatives in the discretized action such that

$$\phi'_j \equiv (\phi_{j+1} - \phi_j)/a_j, \quad (3.6)$$

and similarly for the other fields in the theory. We now construct a 3D theory that reproduces Eq. (3.5), up to differences at the  $j = 1$  and  $N$  boundaries. These differences will be required for a proper holographic interpretation of the deconstructed theory.

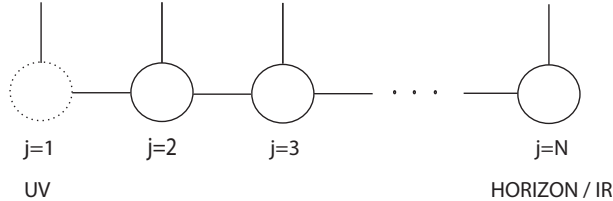


FIG. 1: Moose diagram representation of the deconstructed theory.

Consider a 3D theory with  $N$  global  $U(1)$  symmetries of which  $N - 1$  are gauged. We label the  $N - 1$  gauge factors by the index  $j = 2 \dots N$ . We introduce a set of bi-fundamental complex scalar fields  $\Sigma_j$ ,  $j = 1 \dots N - 1$ , where  $\Sigma_j$  transforms under the  $j^{\text{th}}$  and  $(j + 1)^{\text{th}}$   $U(1)$  factors, with charges  $-1$  and  $+1$ , respectively. In addition, we introduce  $N$  complex scalar fields  $\psi_j$ ,  $j = 1 \dots N$ , where  $\psi_j$  transforms under the  $j^{\text{th}}$   $U(1)$  factor, with charge  $+1$ . The particle content and charge assignments of this theory are conveniently summarized by the moose diagram shown in Fig. 1. The solid circles represent  $U(1)$  gauge groups, while each line connecting to a given circle represents a complex scalar field that transforms under that group. The global  $U(1)$  symmetry is represented by the dotted circle at the left end of the moose.

We assume that the bi-fundamental fields develop vacuum expectation values (vevs)  $\langle \Sigma_j \rangle \equiv v_j$ . Although the first link field  $\Sigma_1$  is charged under the global  $U(1)$  factor, the global symmetry nevertheless remains unbroken if the  $\psi_j$  have vanishing expectation values. This can be seen by noting that the effect of a global phase rotation on  $\langle \Sigma_1 \rangle$  can be undone by a (constant and spatially uniform)  $U(1)$  gauge transformation at the  $j = 2$  site. The effect of this phase rotation on  $\langle \Sigma_2 \rangle$  can then be undone by a  $U(1)$  gauge transformation at the  $j = 3$  site, and so on. In this way, one sees that the global symmetry of the first site remains an invariance of the vacuum, even when the link field vevs assume a nonvanishing profile. We therefore identify the current associated with the global symmetry of the first site as the QED current  $j^\mu$ . As has been discussed in the literature [9], even though the  $U(1)$  symmetry associated with QED is not gauged, the model still describes aspects of superconductivity to the extent that a treatment of electromagnetic fields as external backgrounds is appropriate. In the deconstructed model we could simply add a kinetic term for the associated  $U(1)$  gauge field to describe a fully dynamical electromagnetism, but in order to match the AdS/CFT description we will not do that here.

In order to compute expectation values of  $j^\mu$ , we will turn on a non-propagating gauge field at the first site,  $A_1^\mu$ , that couples to this current. We will also assume that the gauge field at the last site  $A_N^\mu$  is non-propagating and assumes a specified background configuration; this will allow us to impose incoming-wave boundary conditions near the horizon. The boundary fields  $\psi_1$  and  $\psi_N$  are also assumed to be non-propagating below, but only to simplify the discussion. The case in which all the  $\psi_j$  are dynamical is discussed in an appendix.

The Lagrangian for the 3D theory in Fig. 1 is of the form

$$\mathcal{L} = \sum_{j=2}^{N-1} \left[ -\frac{1}{4} (F_{\mu\nu})_j (F^{\mu\nu})_j + Z_j |D_\mu \psi_j|^2 \right] + \sum_{j=1}^{N-1} [|D_\mu \Sigma_j|^2 - Z_j V_j] \quad (3.7)$$

where  $V_j$  determines the scalar potential at the  $j^{\text{th}}$  site. The coefficients  $Z_j$  and the 3D metric  $g_j^{\mu\nu}$  vary from site to site. Although we use the term ‘‘metric’’ to refer to  $g_j^{\mu\nu}$ , the  $g_j^{\mu\nu}$  simply encode the Lorentz-violating couplings of the theory. The covariant derivative is given by

$$D^\mu \Sigma_j = \partial^\mu \Sigma_j + i A_j^\mu \Sigma_j - i A_{j+1}^\mu \Sigma_j, \quad (3.8)$$

and

$$D^\mu \psi_j = \partial^\mu \psi_j - i A_j^\mu \psi_j. \quad (3.9)$$

Notice the absence of  $\psi_j$  and  $A_j$  kinetic terms for  $j = 1$  and  $j = N$  in Eq. (3.7). We identify the non-propagating fields that appear at the ends of the moose with fixed backgrounds in the ultraviolet (UV) and the infrared (IR):

$$\begin{aligned} A_1^\mu &\equiv A_{UV}^\mu(x^\nu), \quad \psi_1 \equiv \psi_{UV}(x^\nu), \\ A_N^\mu &\equiv A_{IR}^\mu(x^\nu), \quad \psi_N \equiv \psi_{IR}(x^\nu). \end{aligned} \quad (3.10)$$

We can now compare Eq. (3.7) to the Lagrangian obtained by latticizing the  $z$  coordinate of the continuum theory, Eq. (3.5). Up to differences that vanish in the  $a \rightarrow 0$  limit, one finds after some algebra that the latticized theory is recovered if one chooses

$$g_j^{00} = \frac{1}{f_j}, \quad g_j^{ab} = -\delta^{ab}, \quad Z_j = \frac{1}{z_j^2} \quad \text{and} \quad v_j = \frac{1}{a_j} \sqrt{\frac{f_j}{2}}, \quad (3.11)$$

the scalar potential

$$V_j = \begin{cases} 2|v_j \psi_{j+1} - \psi_j \Sigma_j|^2 & \text{for } j = 1 \\ 2|v_j \psi_{j+1} - \psi_j \Sigma_j|^2 + m^2 |\psi_j|^2 / z_j^2 & \text{for } j = 2 \dots N - 1 \end{cases} \quad (3.12)$$

and the identification

$$\Sigma_j = v_j \exp[ia_j A_{zj}] \approx v_j(1 + ia_j A_{zj}). \quad (3.13)$$

The potential is not the most general one consistent with the symmetries of the theory; as in any deconstructed model, the form of the action is dictated by the requirement that it reproduce the latticized action obtained from the continuum theory. For example, Eq. (3.12) is fine-tuned so that the  $(\psi'_i)^2$  term in Eq. (3.5) is reproduced when  $\Sigma_j$  is set equal to its vev. For definiteness, we fix the mass parameter  $m^2$  to its holographically motivated value  $m^2 = -2$ . One could allow  $m$  to deviate from this choice in more general theories, but we will not consider that possibility here. The temperature dependence of terms in the action is inferred from the form of  $f_j$ , which depends on temperature via  $z_H = 3/(4\pi T)$ . One could also imagine more general moose models in which the temperature dependence of the  $f_j$  is determined directly from the microscopic properties of the system. Here we will strictly consider the  $f_j$  that follow from discretizing the continuum holographic theory.

In what follows, we work in unitary gauge, corresponding to the gauge  $A_z = 0$  in the four-dimensional theory. As in Eq. (3.13), we ignore the physical fluctuations of the link fields about their vevs. Then, the Lagrangian of the moose model may be written

$$\begin{aligned} \mathcal{L} = & \sum_{j=1}^{N-1} a_j \left[ \frac{1}{2}(\phi'_j)^2 - \frac{f_j}{2}(A'_{a_j})^2 - \frac{f_j}{z_j^2}|\psi'_j|^2 \right] + \sum_{j=2}^{N-1} a_j \left[ \frac{1}{2f_j}(F_{0a})_j^2 - \frac{1}{4}(F_{ab})_j^2 \right] \\ & + \sum_{j=2}^{N-1} a_j \left[ \frac{1}{z_j^2 f_j} |\partial_0 \psi_j - i\phi_j \psi_j|^2 - \frac{1}{z_j^2} |\partial_a \psi_j - iA_{a_j} \psi_j|^2 - \frac{1}{z_j^4} m^2 |\psi_j|^2 \right]. \end{aligned} \quad (3.14)$$

One may now derive the equations of motion for the dynamical fields ( $j = 2 \dots N - 1$ ), assuming the same ansatz applied in the continuum theory. For  $\phi_j$  that are time-independent and spatially constant, the equations of motion for the dynamical fields are given by

$$\phi_j'' - \frac{2}{z_j^2 f_j} \phi_j \psi_j^2 = 0, \quad (3.15)$$

where  $\phi_j'' \equiv (\phi_{j+1} - 2\phi_j + \phi_{j-1})/a^2$ , for  $j = 2 \dots N - 2$  and  $\phi_{N-1}'' \equiv [(\phi_N - \phi_{N-1})/a_H - (\phi_{N-1} - \phi_{N-2})/a]/a_H$ . For the same ansatz, the equations of motion for the  $\psi_j$  are given by

$$\psi_j'' + \frac{1}{a_j} \left( 1 - \frac{z_j^2}{z_{j-1}^2} \frac{f_{j-1}}{f_j} \right) \psi'_{j-1} + \frac{1}{f_j^2} \phi_j^2 \psi_j - \frac{m^2}{z_j^2 f_j} \psi_j = 0, \quad (3.16)$$

where  $\psi_j''$  is defined analogously to  $\phi_j''$  and  $\psi'_j \equiv (\psi_{j+1} - \psi_j)/a_j$ . When  $\phi_j$  is nonvanishing, corresponding to a nonvanishing chemical potential and charge density, the coupling between

$\phi_j$  and  $\psi_j$  in Eq. (3.16) acts as a negative squared mass term for each Cooper pair field  $\psi_j$ , creating an instability that is enhanced for  $z_j$  near  $z_H$  by the temperature-dependent factor of  $1/f_j^2$ .

Finally, we will require the equation of motion for the spatial components of the gauge field, assuming spatially constant fields and the time dependence

$$A_{aj}(x^\mu) \equiv A_{aj} e^{-i\omega t}. \quad (3.17)$$

Again for  $j = 2 \dots N - 1$ , one finds

$$A''_{aj} + \frac{1}{a_j} \left(1 - \frac{f_{j-1}}{f_j}\right) A'_{aj-1} + \left(\frac{\omega^2}{f_j^2} - 2\frac{\psi_j^2}{z_j^2 f_j}\right) A_{aj} = 0, \quad (3.18)$$

where  $A''_j$  and  $A'_j$  are defined analogously to  $\psi''_j$  and  $\psi'_j$ . The exciton fields  $(A_a)_j$  are excited collectively by the external electromagnetic field  $(A_a)_1$ .

The horizon boundary condition on Eqs. (3.15) and (3.16) that correspond to those of the continuum theory are

$$\phi_N = 0 \quad \text{and} \quad \psi'_{N-1} = \frac{2}{3z_N} \psi_N. \quad (3.19)$$

If the  $\psi_N$  field were dynamical at the last site, it turns out that the same boundary condition on  $\psi$  would follow from the  $\psi_N$  equation of motion in the continuum limit, as we discuss in the Appendix. The boundary condition on the spatial components of  $A_N$  can be chosen to reproduce the incoming-wave boundary conditions in the continuum limit, as we discuss in more detail below.

In the continuum holographic theory, physical quantities of interest are related to the values and derivatives of the fields at the UV boundary. In the deconstructed theory, we find that similar relations apply to the expectation value of the charge density  $\rho$  and the current density  $j^a$ , which are identified via their coupling to the background field  $A_{UV}^\mu$ :

$$j^\mu = i \frac{\delta}{\delta A_{UV\mu}} \ln \left\{ \int \prod_{j=2}^{N-1} \mathcal{D}A_j \mathcal{D}\psi_j e^{iS} \right\}. \quad (3.20)$$

This reduces at tree-level to

$$j^\mu = -\frac{\delta}{\delta A_{UV\mu}} S_{cl}[A_{UV}], \quad (3.21)$$

where the dependence on  $A_{UV}$  arises since the fields are evaluated on their classical equations of motion. In the linearized theory, one finds algebraically that  $S_{cl}$  evaluates to a sum of

surface terms

$$S_{cl} = \int d^3x [\mathcal{L}_{UV} + \mathcal{L}_{IR}], \quad (3.22)$$

where the terms involving the exciton fields are given by

$$\mathcal{L}_{UV} = -\frac{1}{2a} \phi_1(\phi_2 - \phi_1) + \frac{1}{2a} f_1 A_{a1}(A_{a2} - A_{a1}) \quad (3.23)$$

and

$$\mathcal{L}_{IR} = -\frac{1}{2a_H} f_{N-1} A_{aN}(A_{aN} - A_{aN-1}), \quad (3.24)$$

using the boundary condition  $\phi_N = 0$ . Before evaluating Eq. (3.21), we first arrange that the IR surface term vanishes. This is consistent with the approach in the continuum holographic theory, where the IR surface term is also present, but is simply discarded [30]. To eliminate Eq. (3.24), we can add an *ad hoc* term to the Lagrangian such that the desired IR boundary condition is consistent with vanishing IR surface term. Near the horizon, the ingoing-wave solution satisfies Eq. (2.15), which can be imposed as a boundary condition in the deconstructed model in a number of ways. We choose to approximate the ingoing-wave boundary condition as

$$A'_{aN-n-1} = \frac{i\omega}{f_{N-n-1}} A_{aN-n} \quad (3.25)$$

for some  $n$ , with  $n \ll N$  in the continuum limit  $N \rightarrow \infty$ . If  $n$  is taken too small, the factor of  $1/f$  in Eq. (3.25) is large and magnifies the discrepancy between the discretized and continuum boundary conditions. Integrating from  $j = n$  towards the horizon and solving the  $\omega^2$ -dependent equations of motion, one obtains a relation between  $A_{aN}$  and  $A_{aN-1}$  that generally leads to a nonvanishing surface term. However, if we add a new term to the Lagrangian of the form

$$\mathcal{L}_H = \xi [c(\omega^2)A_{aN} - A_{aN-1}]^2, \quad (3.26)$$

then the new IR surface term, evaluated on the solution to the equations of motion, becomes a function of  $c(\omega^2)$ . This function can be chosen so that the surface term vanishes. Eq. (3.26) can be expressed as a function of the gauge-invariant field strength tensors  $F_{xzN-1}$  and  $F_{0xN-1}$ , and the function  $c(\omega^2)$  may be interpreted as a function of  $-\partial_t^2$ , which ultimately acts on the non-dynamical field  $A_{aN}$ . The function  $c(\omega^2)$  may be replaced by a polynomial approximation, valid at least over some finite range in  $\omega$ . In this way, our discrete approximation to the ingoing-wave boundary condition, Eq. (3.25), can be imposed  $n$  sites away from the IR boundary, while the IR surface term is arranged to vanish.

The expectation value of the current thus depends only on the UV surface terms, as in the continuum holographic theory. Each  $j = 2$  field in Eq. (3.23) can be related to the corresponding boundary field by the discrete version of a bulk-to-boundary propagator. For example, we could write  $\phi_j = B_{j1}\phi_1$ , for some bulk-to-boundary propagator  $B_{j1}$ . Then the charge density is found by computing

$$\rho = \frac{\delta}{\delta\phi_1} \left[ -\frac{1}{2a}\phi_1^2 (B_{21} - 1) \right] = -\frac{1}{a}\phi_1 (B_{21} - 1). \quad (3.27)$$

The quantity  $\phi_1(B_{21} - 1)/a$  is nothing more than what we would find by numerically solving the  $\phi$  equation of motion and evaluating  $\phi_1'$  as we defined it previously. Hence, we conclude

$$\rho = -\phi_1', \quad (3.28)$$

in agreement with the holographic prescription for computing the charge density in the continuum theory. By the same reasoning, the current density following from Eq. (3.23) is given by

$$j^a = -f_1 A'_{a1}, \quad (3.29)$$

which also agrees with the usual holographic prescription in the continuum, where  $f_1 \rightarrow 1$ . Since  $j^0$  is proportional to the charge density operator, we identify  $\phi_1$  with the chemical potential

$$\mu = \phi_1. \quad (3.30)$$

The transition to the superconducting phase occurs when the  $\psi_j$  develop a nonvanishing profile. In the continuum limit,  $\psi(z)$  takes the form  $\psi(z) = \psi^{(1)}z + \psi^{(2)}z^2$  near the UV boundary, so that the existence of the condensate is determined by nonvanishing first or second derivatives:

$$\psi^{(1)} \equiv \psi'(z=0) \neq 0 \quad \text{or} \quad \psi^{(2)} \equiv \frac{1}{2}\psi''(z=0) \neq 0, \quad (3.31)$$

In the discretized theory, we use the analogous expression  $\psi_j = \psi^{(1)}z_j + \psi^{(2)}z_j^2$  evaluated at the first two lattice sites ( $z_1 = \epsilon$  and  $z_2 = \epsilon + a$ ) to define the operators  $\psi^{(1)}$  and  $\psi^{(2)}$ ,

$$\psi^{(1)} = \frac{\psi_2 \epsilon^2 - \psi_1(\epsilon + a)^2}{\epsilon^2(\epsilon + a) - \epsilon(\epsilon + a)^2} \quad \text{and} \quad \psi^{(2)} = \frac{\psi_2 \epsilon - \psi_1(\epsilon + a)}{\epsilon(\epsilon + a)^2 - \epsilon^2(\epsilon + a)}. \quad (3.32)$$

These definitions have the appropriate continuum limit. As in Sec. II, we restrict ourselves to the case where  $\psi^{(1)} = 0$  and we define the order parameter to be  $\langle O_2 \rangle \equiv \sqrt{2}\psi^{(2)}$ , following



the conventions of Ref. [9]. Although  $\psi^{(1)}$  and  $\psi^{(2)}$  do not have the same holographic interpretation in the deconstructed theory away from the continuum limit, our definitions provide an accurate measure of whether a nonvanishing profile of the  $\psi_j$  has been dynamically generated.

#### IV. RESULTS

In this section, we numerically solve the discretized theory of Sec. III for  $N \in \{5, 10, 100, 1000\}$ . In the case of  $N = 1000$ , for the purpose of connecting with the continuum theory, we fix the UV cutoff  $z_1 = \epsilon = 10^{-1}$ , while for other  $N$  we set  $\epsilon = a$ , the bulk lattice spacing. We fix the lattice spacing at the horizon  $a_H = 10^{-5}$ . In all cases, we impose the following boundary conditions:

$$\phi'_1 = -\rho = -1, \quad \psi^{(1)} = 0, \quad \phi_N = 0, \quad \text{and} \quad \psi'_{N-1} = \frac{2}{3z_N}\psi_N, \quad (4.1)$$

where we have used the scaling symmetry of the theory to fix  $T_c$  by setting  $\rho = 1$ . Searching for nonvanishing  $\psi_j$  solutions as we vary the temperature, we find there is a critical temperature for each  $N$  at which the operator  $\langle O_2 \rangle$  condenses, as shown in Fig. 2. We note that there are numerous non-zero solutions for  $\psi_j$  but, as in the continuum model [9], we retain only the monotonic solutions. For  $N = 5$ ,  $N = 10$ ,  $N = 100$ , and  $N = 1000$  we find the critical temperatures  $T_c = 0.076 \rho^{1/2}$ ,  $T_c = 0.088 \rho^{1/2}$ ,  $T_c = 0.111 \rho^{1/2}$ , and  $T_c = 0.118 \rho^{1/2}$  respectively. Here we reintroduced the factor of  $\rho^{1/2}$  as indicated by the scaling relations. It is interesting to see that for all  $N$  we retain the square root behavior of the phase transition. We find that the curves in Fig. 2 near  $T_c$  are well fit by the form  $\langle O_2 \rangle = C_N T_c^2 (1 - T/T_c)^{1/2}$ . The values we obtain for the coefficients are  $C_{1000} = 127$ ,  $C_{100} = 20$ ,  $C_{10} = 58$ , and  $C_5 = 93$ , as compared to the continuum value  $C = 144$  [9].

We would also like to study the behavior of the complex conductivity away from the continuum limit. Using the expression for the current Eq. (3.29), we find the following expression for the conductivity:

$$\sigma = \frac{j^x}{E_x} = \frac{j^x}{\dot{A}_x} = -\frac{if_1(A_{x2} - A_{UVx})/a}{\omega A_{UVx}}. \quad (4.2)$$

As discussed in Sec. III, we impose the ingoing-wave boundary condition, Eq. (3.25),  $n$  sites

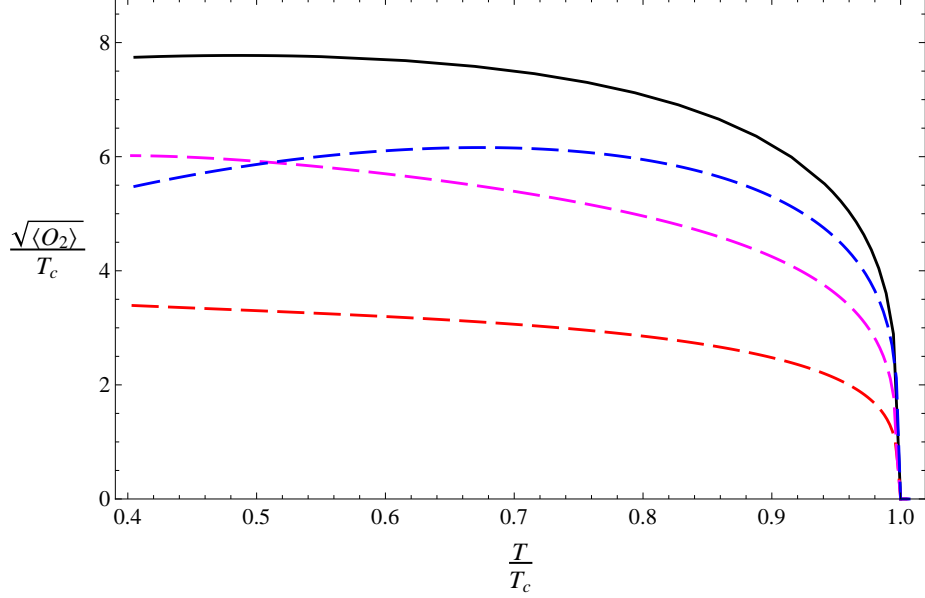


FIG. 2: This figure displays the condensation phase transition at critical temperature  $T = T_c$ . The top curve is the  $N = 1000$  curve and below that the dashed curves from top to bottom around  $T_c$  are  $N = 5$ ,  $N = 10$ , and  $N = 100$ , respectively. The 1000-site curve includes a fixed UV cutoff  $\epsilon$ , which allows for a smooth continuum limit.

away from the horizon. In particular, we set

$$A_{x_{N-n}} = 1 \quad \text{and} \quad A_{x_{N-n-1}} = 1 - \frac{i\omega a}{f_{N-n-1}}, \quad (4.3)$$

where we have fixed the arbitrary normalization  $A_{x_{N-n}} = 1$ . Our choices for the shift  $n$  for  $N = 1000, 100, 10$  and  $5$  are  $n = 20, 10, 2$  and  $2$ , respectively. With these boundary conditions for  $A_{x_j}$  we compute the real and imaginary parts of  $\sigma$ , as shown in Figs. 3 and 4. It is important to note that the graphs of  $\text{Im}[\sigma(\omega)]$  in the superconducting phase exhibit a simple pole at  $\omega = 0$ . This implies the presence of a delta function contribution to the real part,  $\text{Re}[\sigma(\omega)] \propto \delta(\omega)$ , as discussed in Sec. II. For  $N = 10$  there are a series of peaks in  $\text{Re}[\sigma(\omega)]$  with a corresponding pole-like structure in the imaginary part as follows from the Kramers-Kronig relation Eq. (2.17). Finally, the oscillatory behavior of  $\text{Re}[\sigma(\omega)]$  at large  $\omega$  displayed in the  $N = 100$  and  $N = 1000$  plots is consistent with our expectation from Eq. (2.19) given that our boundary condition is only approximately ingoing wave.

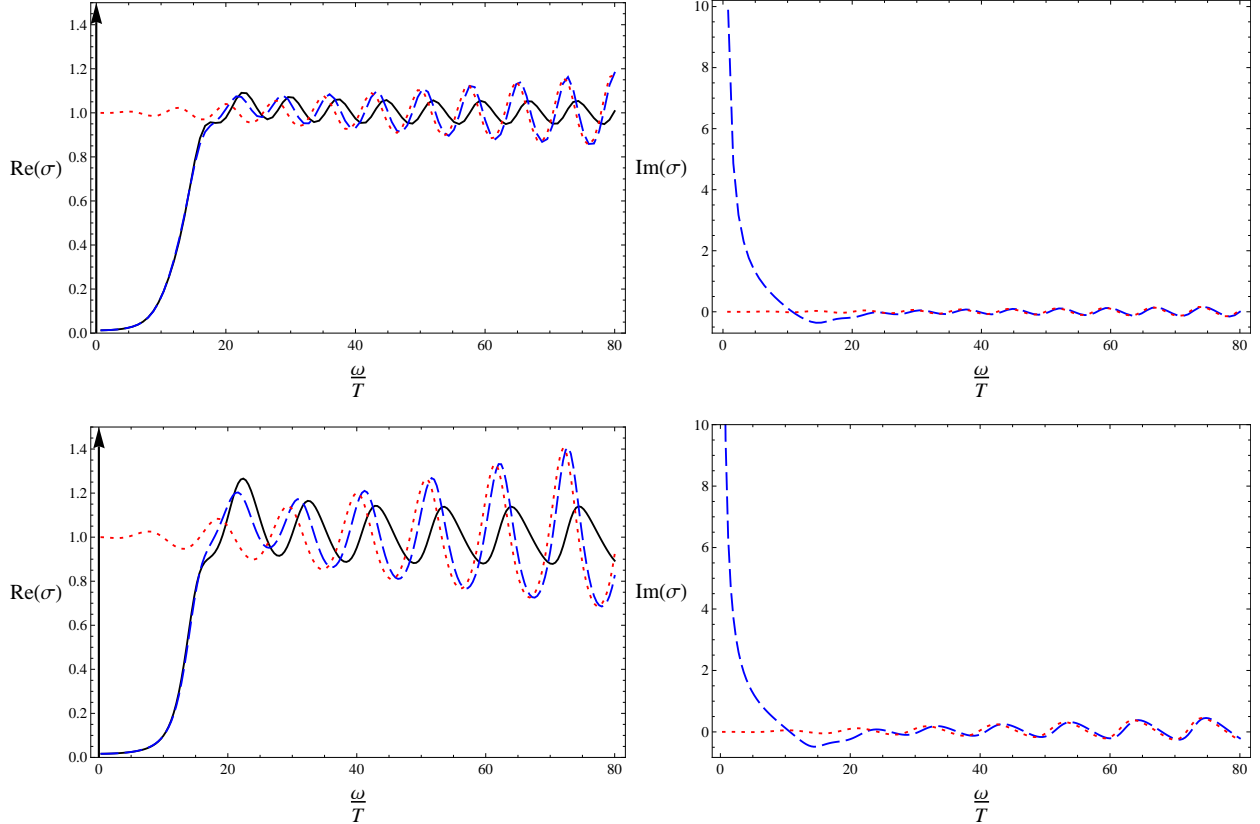


FIG. 3: Complex conductivities. The  $(N, T/T_c)$  values for the top and bottom rows are given by  $(1000, 0.55)$  and  $(100, 0.53)$ , respectively. The dotted (red) curve is the normal (n) phase while the dashed (blue) curve is the superconducting (sc) phase. The vertical arrow represents a delta function. The solid (black) curve is the ratio:  $\text{Re}(\sigma_{\text{sc}})/\text{Re}(\sigma_{\text{n}})$ .

## V. CONCLUSIONS

Dimensional deconstruction is a powerful technique for finding lower-dimensional theories that share some of the interesting phenomenological features of their higher-dimensional progenitors. In this paper, we have considered the dimensional deconstruction of four-dimensional holographic theories of superconductivity. We have shown how the AdS/CFT prescriptions for computing physical quantities of interest (for example, charge densities and currents) emerge in the lower-dimensional, discretized theory. We have also demonstrated that deconstructed theories with a relatively small number of lattice sites (here taken  $\geq 5$ ) do indeed retain enough of the physics of the continuum limit to provide possible models of superconductivity on their own.

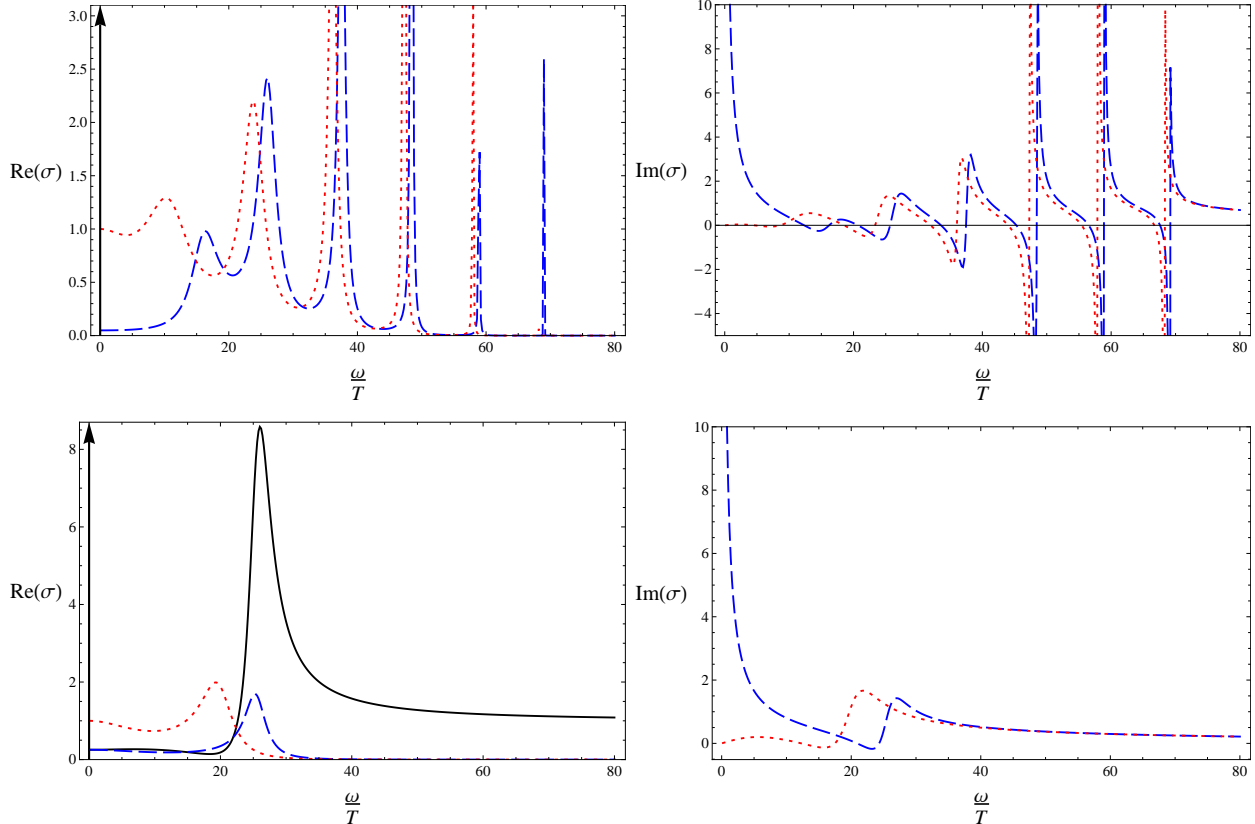


FIG. 4: Complex conductivities. The  $(N, T/T_c)$  values for the top and bottom rows are given by  $(10, 0.54)$  and  $(5, 0.50)$ , respectively. The dotted (red) curve is the normal (n) phase while the dashed (blue) curve is the superconducting (sc) phase. The vertical arrow represents a delta function. The solid (black) curve (omitted for  $N = 10$ , for clarity) is the ratio:  $\text{Re}(\sigma_{sc})/\text{Re}(\sigma_n)$ .

We view the results of this work as preliminary, in the sense that we have only considered the deconstruction of one of the simplest, s-wave holographic superconductors that were proposed in the first papers on the application of the AdS/CFT correspondence to this problem. Much of what we have found in the present work leads to questions and suggestions for future study:

- Dimensional deconstruction also motivates new models of  $p$ - and  $d$ -wave superconductors. It would be interesting to study the phenomenology of those models.
- In the present approach, the photon field is not included as a dynamical degree of freedom in the deconstructed theory. However, the theory can be easily modified by gauging the electromagnetic U(1) symmetry and adding an associated gauge kinetic

term.

- The deconstructed model suggests the possibility of hidden local symmetries in the interactions between Cooper pairs and excitons. Perhaps absorption studies would be able to test the existence of these states and interactions.
- If one deviates from a strict matching to the continuum holographic theory, then one has greater freedom in constructing a model that is based on a very small number of replicated gauge groups (for example, two or three). Would a two- or three-site model of superconductivity be phenomenologically viable?
- The deconstructed model introduces temperature-dependent couplings inferred by a holographic model. It would be important to deduce these couplings instead from a microscopic description.
- In the present work, the fluctuations of the link fields were ignored, consistent with the tacit assumption that these fields are heavy. However, these fields, which have no counterpart in the continuum holographic theory, might also have a physical interpretation.

We look forward to considering these issues in more detail in future work.

## Acknowledgments

We thank Henry Krakauer, Enrico Rossi and Christopher Triola for useful conversations. This work was supported by the NSF under Grant PHY-1068008. In addition, C.D.C. thanks Joseph J. Plumeri II for his generous support.

## Appendix A: A purely dynamical $\psi$

To simplify our discussion, it was assumed earlier that the  $\psi_j$  fields at the ends of the moose,  $\psi_1$  and  $\psi_N$ , were background fields. Here we show that the same boundary conditions would be obtained in the continuum limit if we allow all the  $\psi_j$  to be dynamical fields. The Lagrangian that is relevant in this case is a minor modification of Eq. (3.14); the third sum in this expression, which runs from  $j = 2$  to  $N - 1$ , is changed to one which runs from  $j = 1$

to  $N$  (with  $a_N = a_H$ ) for the first two terms in square brackets and from  $j = 2$  to  $N$  for the mass squared term. We also shift  $z_N$  away from its previous value by  $\epsilon_H$ , which serves as a cutoff to regulate the divergence in  $1/f_N$ . Eq. (3.16) remains unaltered, but now there are two additional equations of motion, for  $\psi_1$  and  $\psi_N$ :

$$\frac{1}{a}\psi'_1 + \frac{1}{f_1^2}\phi_1^2\psi_1 = 0, \quad (\text{A1})$$

and

$$-\frac{1}{a_H}\psi'_{N-1} + \frac{z_{N-1}^2}{z_N^2 f_N f_{N-1}}\phi_N^2\psi_N + \frac{2z_{N-1}^2}{f_{N-1}z_N^4}\psi_N = 0, \quad (\text{A2})$$

where  $\psi'_{N-1} = (\psi_N - \psi_{N-1})/a_H$ . These equations can be viewed as dictating the boundary conditions for Eq. (3.14), which, in our previous approach, were chosen freely to mimic the boundary conditions of the continuum theory. Eq. (A1) reduces in the continuum limit to the boundary condition  $\psi'_1 = 0$ . Since  $\phi_N \equiv 0$ , the second term in Eq. (A2) vanishes ( $1/f_N$  is finite for finite cutoff  $\epsilon_H$ ). Hence,

$$\psi'_{N-1} = \left[ \frac{2a_H z_{N-1}^2}{f_{N-1} z_N^4} \right] \psi_N. \quad (\text{A3})$$

The quantity in brackets can be expanded in powers of  $a_H$  while maintaining  $\epsilon_H \ll a_H$ ; one finds

$$\psi'_{N-1} = \left[ \frac{2}{3z_H} - \frac{2}{3z_H^2}a_H + \mathcal{O}(a_H^2) \right] \psi_N. \quad (\text{A4})$$

In the limit  $a_H \rightarrow 0$  we recover the boundary condition in Eq. (3.19). In summary, the effect of treating the  $\psi_j$  as dynamical fields everywhere is to modify the form of the boundary conditions away from those of the continuum limit:

$$\psi'_1 = -\frac{a}{f_1^2}\phi_1^2\psi_1, \quad \text{and} \quad \psi'_{N-1} = \left[ \frac{2}{3z_H} - \frac{2}{3z_H^2}a_H \right] \psi_N. \quad (\text{A5})$$

- 
- [1] J. G. Bednorz and K. A. Muller, Z. Phys. B **64**, 189 (1986).
  - [2] W. L. McMillan, Phys. Rev. **167**, 331 (1968).
  - [3] J. W. Loram, K. A. Mirza, J. R. Cooper and W. Y. Liang, Phys. Rev. Lett. **71**, 1740 (1993);  
T. Timusk and B. Statt, Rep. Prog. Phys. **62**, 1 (1999).
  - [4] Z. A. Xu, *et al.*, Nature **406**, 486 (2000).
  - [5] Y. Kamihara, T. Watanabe, M. Hirano and H. Hosono, J. Am. Chem. Soc. **130**, 11 (2008).

- [6] H. B. Nielsen and P. Olesen, Nucl. Phys. B **61**, 45 (1973).
- [7] J. M. Maldacena, Adv. Theor. Math. Phys. **2**, 231 (1998) [hep-th/9711200]; E. Witten, Adv. Theor. Math. Phys. **2**, 253 (1998) [arXiv:hep-th/9802150]; S. S. Gubser, I. R. Klebanov and A. M. Polyakov, Phys. Lett. B **428**, 105 (1998) [arXiv:hep-th/9802109].
- [8] S. S. Gubser, Phys. Rev. D **78**, 065034 (2008) [arXiv:0801.2977 [hep-th]].
- [9] S. A. Hartnoll, C. P. Herzog and G. T. Horowitz, Phys. Rev. Lett. **101**, 031601 (2008) [arXiv:0803.3295 [hep-th]]; S. A. Hartnoll, C. P. Herzog and G. T. Horowitz, JHEP **0812**, 015 (2008) [arXiv:0810.1563 [hep-th]].
- [10] S. S. Gubser and S. S. Pufu, JHEP **0811**, 033 (2008) [arXiv:0805.2960 [hep-th]]; M. Ammon, J. Erdmenger, V. Grass, P. Kerner and A. O'Bannon, Phys. Lett. B **686**, 192 (2010) [arXiv:0912.3515 [hep-th]]; R. -G. Cai, Z. -Y. Nie and H. -Q. Zhang, Phys. Rev. D **82**, 066007 (2010) [arXiv:1007.3321 [hep-th]]; J. -W. Chen, Y. -J. Kao, D. Maity, W. -Y. Wen and C. -P. Yeh, Phys. Rev. D **81**, 106008 (2010) [arXiv:1003.2991 [hep-th]]; F. Benini, C. P. Herzog and A. Yarom, Phys. Lett. B **701**, 626 (2011) [arXiv:1006.0731 [hep-th]].
- [11] S. A. Hartnoll and C. P. Herzog, Phys. Rev. D **77**, 106009 (2008) [arXiv:0801.1693 [hep-th]].
- [12] S. A. Hartnoll, J. Polchinski, E. Silverstein and D. Tong, JHEP **1004**, 120 (2010) [arXiv:0912.1061 [hep-th]].
- [13] G. T. Horowitz, arXiv:1002.1722 [hep-th].
- [14] C. C. Homes *et al.*, Nature **430**, 539 (2004).
- [15] J. Erdmenger, P. Kerner and S. Muller, arXiv:1206.5305 [hep-th].
- [16] G. T. Horowitz and M. M. Roberts, JHEP **0911**, 015 (2009) [arXiv:0908.3677 [hep-th]].
- [17] C. P. Herzog, J. Phys. A A **42**, 343001 (2009) [arXiv:0904.1975 [hep-th]];
- [18] S. A. Hartnoll, Class. Quant. Grav. **26**, 224002 (2009) [arXiv:0903.3246 [hep-th]];
- [19] N. Arkani-Hamed, S. Dimopoulos and G. R. Dvali, Phys. Lett. B **429**, 263 (1998) [hep-ph/9803315]; I. Antoniadis, N. Arkani-Hamed, S. Dimopoulos and G. R. Dvali, Phys. Lett. B **436**, 257 (1998) [hep-ph/9804398].
- [20] L. Randall and R. Sundrum, Phys. Rev. Lett. **83**, 3370 (1999) [hep-ph/9905221]; L. Randall and R. Sundrum, Phys. Rev. Lett. **83**, 4690 (1999) [hep-th/9906064].
- [21] H. Davoudiasl, J. L. Hewett and T. G. Rizzo, Phys. Rev. Lett. **84**, 2080 (2000) [hep-ph/9909255]; L. J. Hall and C. F. Kolda, Phys. Lett. B **459**, 213 (1999) [hep-ph/9904236].
- [22] K. R. Dienes, E. Dudas and T. Gherghetta, Phys. Lett. B **436**, 55 (1998) [hep-ph/9803466];

- K. R. Dienes, E. Dudas and T. Gherghetta, Nucl. Phys. B **537**, 47 (1999) [hep-ph/9806292].
- [23] N. Arkani-Hamed, A. G. Cohen and H. Georgi, Phys. Rev. Lett. **86**, 4757 (2001) [hep-th/0104005]; C. T. Hill, S. Pokorski and J. Wang, Phys. Rev. D **64**, 105005 (2001) [hep-th/0104035].
- [24] N. Arkani-Hamed, A. G. Cohen and H. Georgi, Phys. Lett. B **513**, 232 (2001) [hep-ph/0105239]; N. Arkani-Hamed, A. G. Cohen, T. Gregoire and J. G. Wacker, JHEP **0208**, 020 (2002) [hep-ph/0202089]; N. Arkani-Hamed, A. G. Cohen, E. Katz, A. E. Nelson, T. Gregoire and J. G. Wacker, JHEP **0208**, 021 (2002) [hep-ph/0206020]; C. Csaki, J. Erlich, C. Grojean and G. D. Kribs, Phys. Rev. D **65**, 015003 (2002) [hep-ph/0106044]; S. Dimopoulos, D. E. Kaplan and N. Weiner, Phys. Lett. B **534**, 124 (2002) [hep-ph/0202136].
- [25] M. Bando, T. Kugo, S. Uehara, K. Yamawaki and T. Yanagida, Phys. Rev. Lett. **54**, 1215 (1985); R. Casalbuoni, S. De Curtis, D. Dominici and R. Gatto, Phys. Lett. B **155**, 95 (1985).
- [26] J. Frenkel, Phys. Rev. **37**, 17 (1931).
- [27] D. T. Son and M. A. Stephanov, Phys. Rev. D **69**, 065020 (2004) [hep-ph/0304182].
- [28] I. R. Klebanov and E. Witten, Nucl. Phys. B **556**, 89 (1999) [hep-th/9905104]; V. Balasubramanian, P. Kraus and A. E. Lawrence, Phys. Rev. D **59**, 046003 (1999) [hep-th/9805171]; V. Balasubramanian, P. Kraus, A. E. Lawrence and S. P. Trivedi, Phys. Rev. D **59**, 104021 (1999) [hep-th/9808017].
- [29] J. D. Jackson, *Classical Electrodynamics*, Third Edition, Wiley (1998).
- [30] D. T. Son and A. O. Starinets, JHEP **0209**, 042 (2002) [hep-th/0205051].